Supporting Information

Effective Phagocytosis of Low Her2 Tumor Cell Lines with Engineered, Aglycosylated IgG Displaying High FcγRIIa Affinity and Selectivity

Sang Taek Jung[a,b,1], William Kelton[a,1], Tae Hyun Kang[c], Daphne T.W. Ng[d], Jan Terje Andersen[e,f], Inger Sandlie[e,f], Casim A. Sarkar[d,g], & George Georgiou[a,c,h,i,2]

[a]Department of Chemical Engineering, [c]Department of Biomedical Engineering, [h]Section of Molecular Genetics and Microbiology, [i]Institute for Cellular and Molecular Biology, University of Texas at Austin, Austin, TX 78712, USA, [b]Department of Bio and Nano Chemistry, Kookmin University, Seoul, Republic of Korea, [d]Department of Bioengineering, [g]Department of Chemical & Biomolecular Engineering, University of Pennsylvania, Philadelphia, PA 19104, USA, [e]Centre for Immune Regulation (CIR) and Department of Molecular Biosciences, University of Oslo, 0316 Oslo, Norway, [f]CIR and Department of Immunology, Rikshospitalet University Hospital, N-0424 Oslo, Norway.

[1]S.T.J. and W.K. contributed equally to this work.

[2]To whom correspondence should be addressed. E-mail: gg@che.utexas.edu; Telephone: 512-471-6975; Fax: 512-471-7963.

SI Materials and Methods. Molecular Biology Techniques: All plasmids and primers used in this study are described in supplementary Table S1 and Table S2. A gene encoding the human IgG1 Fc (comprising the hinge, CH2, and CH3 domains (*1*)), was ligated into pPelBFLAG on SfiI restriction endonuclease sites to generate pPelBFLAG-Fc. To construct pTrc99A-DsbA-Fc2a-FLAG, the Fc2a gene containing mutations S298G and T299A in the CH2 region was PCR amplified using two primers (STJ#422 and STJ#147) with the template pTrc99A-DsbA-Fc-FLAG (*1*), and ligated into SacII / HindIII restriction enzyme-treated pTrc99A-DsbA-Fc-FLAG. For the construction of pSTJ4-AglycoT-Fc2a, the Fc2a gene was amplified by primers STJ#290 and STJ#291, with pTrc99A-DsbA-Fc2a-FLAG as a template. The amplified PCR fragments were ligated into SalI / EcoRV digested pSTJ4-AglycoT to generate pSTJ4-AglycoT-Fc2a. pSTJ4-AglycoT-Fc5-2a (E382V/M428I/S298G/T299A) was generated by amplifying the Fc5-2a gene using two primers (STJ#490 and STJ#220) and pSTJ4-AglycoT-Fc5 as a template, followed by SacII / EcoRI restriction enzyme digestion, and ligation into digested pSTJ4-AglycoT.

Trastuzumab heavy chains encoding either wild type human Fc or the Fc5, Fc2a, or Fc5-2a mutants were amplified using the primers STJ#474 and STJ#67 with the respective templates pSTJ4-AglycoT, pSTJ4-AglycoT-Fc5, pSTJ4-AglycoT-Fc2a, or pSTJ4-AglycoT-Fc5-2a. Each fragment was ligated into the pPelBFLAG vector using the *Sfi*I restriction enzyme sites to generate pPelB-AglycoT(H)-FLAG, pPelB-AglycoT(H)-Fc5-FLAG, pPelB-AglycoT(H)-Fc2a-FLAG, and pPelB-AglycoT(H)-Fc5-2a-FLAG. pBADNlpAHis-M18 was constructed by ligating the NlpA fused M18 scFv gene amplified from pMoPac1-FLAG-

M18 (*2*), and digested with *Xba*I–*Hin*dIII restriction enzymes, into pBAD30-KmR (*2*) digested with the same restriction endonucleases. Ligation of the trastuzumab VL-Cκ gene, amplified using two primers (STJ#475 and STJ#476) and template pSTJ4-AglcoT, into pBADNlpAHis-M18 using *Sfi*I restriction sites generated pBADNlpA-VL-Cκ-His. The PelB leader peptide-fused trastuzumab VL-Cκ gene was amplified with primers STJ#16 and STJ#340 from pSTJ4-AglycoT as the template, digested with *Xba*I / *Hin*dIII endonucleases, and ligated into pBADNlpA-VL-Cκ-His digested with the same endonucleases to generate pBADPelB-VL-Cκ. pBAD-AglycoT(L)-His was constructed by ligating *Xba*I digested PCR fragments amplified using the primers STJ#70 and STJ#332 with pBADPelB-VL-Cκ as a template into *Xba*I digested pBADNlpA-VL-Cκ-His.

The Fc1001, Fc1002, Fc1003, Fc1004, FcG236A, and FcN297D genes were PCR amplified from AglycoT(H)-Fc1001-FLAG, AglycoT(H)-Fc1002-FLAG, AglycoT(H)-Fc1003-FLAG, AglycoT(H)-Fc1004-FLAG, AglycoT(H)-FcG236A-FLAG, and AglycoT(H)-FcN297D-FLAG, respectively by using the primers STJ#290 and STJ#498, then digested with *Sal*I and *Xba*I restriction enzymes, and ligated into the mammalian expression vector, pMAZ-IgH-GlycoT (*1*), to generate pMAZ-IgH-GlycoT-Fc1001, pMAZ-IgH-GlycoT-Fc1002, pMAZ-IgH-GlycoT-Fc1003, pMAZ-IgH-GlycoT-Fc1004, pMAZ-IgH-GlycoT-FcG236A, and pMAZ-IgH-GlycoT-FcN297D, respectively.

For 2B6-N297D gene synthesis (*3*), 2B6 variable domains from heavy and light chains were gene assembled by PCR with Phusion polymerase (New England Biolabs) from primers WK#158 – WK#169 for the light chain and WK#172 – WK#187 for the heavy

chain (25 cycles with 98 ^{o}C denaturation 1 min, 55 ^{o}C denaturation 1 min and 72 ^{o}C extension 2 min were performed before a 10 min final extension step). Correctly assembled genes were amplified with the light chain primers WK#158, WK#170 and heavy chain primers WK#171, WK#187 by overlap extension (OLE) PCR (*4*). Briefly, the megaprimer generated in the previous step was added with Phusion polymerase at a 1:250 molar ratio to heavy chain template (pMAZ-IgH-GlycoT-FcN297D) and light chain template (pMAZ-IgL-GlycoT) (25 cycles of amplification were performed with 98 ^{o}C denaturation 1 min, 55 ^{o}C denaturation 1 min and 72 ^{o}C extension 10 min steps). Remaining template plasmid in the PCR reaction was digested with Dpn1 endonuclease for 1 h at 37 ^{o}C and the final mixture was transformed into Jude-1 cells (F' [Tn*10(*Tet^{r}*)* proAB^{+} *lacI*^{q} Δ(*lacZ*)M15] *mcrA* Δ(*mrr-hsdRMS-mcrBC*) 80d*lac*ZΔM15 Δ*lacX74 deoR recA1 araD139* Δ(*ara leu*)7697 *galU galK rpsL endA1 nupG*) (*5*).

pMAZ-FcγRIIa$_{H131}$-GST was cloned by the OLE PCR method as described above using a megaprimer generated with primers WK#100 and WK#101 from pDNR-LIB-FcγRIIa (ATCC: MGC-23887). The second PCR step cloned this megaprimer fragment in place of FcγRI in pMAZ-FcγRI-GST, a plasmid derived by OLE PCR from pMAZ-IgH GlycoT by cloning the FcγRI-GST cassette from pcDNA3(oriP)-FcγRI (*6*) with primers WK#56 and WK#57. pMAZ-FcγRIIa$_{R131}$-GST was generated by OLE PCR using pMAZ-FcγRIIa$_{H131}$-GST as a template to generate a megaprimer with primers (WK#100 and WK#116).

For the construction of pPelBHis-FcγRIIIa$_{V158,}$ the FcγRIIIa$_{V158}$ gene was PCR amplified using primers STJ#76 and STJ#82 and the template pCMV-SPORT6-FcγRIIIa (ATCC: MGC-

45020), and then ligated into pPelBHis (*1*) using the *Sfi*I sites. pMAZ-FcγRIIIa$_{V158}$-GST was cloned by OLE PCR from pMAZ-FcγRIIIa$_{V158}$, a monomeric mammalian derivative of pPelBHis-FcrRIIIa$_{V158}$, with primers WK#91 and WK#92 used to generate the megaprimer. The recipient vector was pMAZ-FcγRIIa$_{H158}$-GST. pMAZ-FcγRIII$_{F158}$-GST was likewise cloned by OLE PCR from pMAZ-FcγRIIIa$_{V158}$-GST with primers WK#91 and WK#94 used for megaprimer synthesis and pMAZ-FcγRIIIa$_{V158}$-GST as the recipient vector.

***IgG Display in E. coli for FcγR Binding*.** pBAD-AglycoT(L)-His was transformed with either pPelB-AglycoT(H)-FLAG, pPelB-AglycoT(H)-Fc5-FLAG, pPelB-AglycoT(H)-Fc2a-FLAG, or pPelB-AglycoT(H)-Fc5-2a-FLAG for wild type trastuzumab, trastuzumab-Fc5, trastuzumab-Fc2a, or trastuzumab-Fc5-2a, respectively into *E. coli* JUDE-1. The transformed *E. coli* cells were cultured overnight at 37 °C with 250 rpm shaking in TB (Terrific Broth; Becton Dickinson Diagnostic Systems Difco™) supplemented with 2% (wt/vol) glucose, chloramphenicol (40 µg/ml) and kanamycin (50 µg/ml). The overnight cultured cells were diluted 1:100 in fresh 7 ml of TB medium with chloramphenicol (40 µg/ml) and kanamycin (50 µg/ml) in 125 ml Erlenmeyer flask. After incubation at 37 °C for 2 h and cooling at 25 °C for 20 min with 250 rpm shaking, protein expression was induced with 1 mM of isopropyl-1-thio-D-galactopyranoside (IPTG). 20 h after IPTG induction, 6 ml of the culture broth was harvested by centrifugation and washed two times in 1 ml of cold 10 mM Tris-HCl (pH 8.0). After re-suspension in 1 ml cold STE solution (0.5 M Sucrose, 10 mM Tris-HCl, 10 mM EDTA, pH 8.0), the cells were incubated

at 37 °C for 30 min on a tube rotator, pelleted by centrifugation at 12,000 x g for 1 min and washed in 1 ml of cold Solution A (0.5 M Sucrose, 20 mM $MgCl_2$, 10 mM MOPS, pH 6.8). The washed cells were incubated in 1 ml Solution A with 1 mg/ml of hen egg lysozyme at 37 °C for 15 min. After centrifugation at 12,000 x g for 1 min, the resulting spheroplast pellets were resuspended in 1 ml of cold PBS. 300 µl of the spheroplasts were further diluted in 700 µl of PBS and labeled with 30 nM FcγRI-FITC to analyze binding. For FACS analysis of FcγRIIa binding, spheroplasts were incubated with 30 nM FcγRIIa C-terminal fused to GST (*6*), washed in 1 ml of PBS, and labeled with polyclonal goat anti-GST-FITC (Abcam) diluted 1:200 in 1 ml of PBS. After incubation for 1 h with vigorous shaking at 25 °C protected from light, the mixture was pelleted by centrifugation at 12,000 x g for 1 min and resuspended in 1 ml of PBS. The fluorescently labeled spheroplasts were diluted in 2.5 ml of PBS and analyzed on BD FACSCalibur (BD Bioscience).

Library Construction. An error prone PCR library using the trastuzumab-CH2-CH3 region of Fc5-2a as a template was created using standard techniques (*7*) and the two primers STJ#485 and STJ#67. VH-CH1 was then PCR amplified using the primers STJ#474 and STJ#486 from the template (pSTJ4-AglycoT). The two fragments, hinge-CH2-CH3 regions and VH-CH1 regions, were assembled by gene assembly PCR using the primers STJ#474 and STJ#67 to generate the trastuzumab heavy chain (VH-CH1-Hinge-CH2-CH3) library. The amplified heavy chain library genes were ligated into SfiI-digested pPelBFLAG. The resulting plasmids were transformed into E. coli Jude-1 harboring the light chain plasmid

(pBAD-AglycoT(L)-His).

Culture and Spheroplasting of E. coli for Library Screening. For screening, *E. coli* Jude-1 cells containing the heavy chain plasmid (pPelB-VH-CH1-Hinge-CH2-CH3) and the light chain plasmid (pBAD-AglycoT(L)-His) were cultured overnight at 37 °C with 250 rpm shaking in TB supplemented with 2% (w/v) glucose and appropriate antibiotics (40 µg/ml of chloramphenicol and 50 µg/ml of kanamycin). The overnight cultured cells were diluted 1:100 in 110 ml of fresh TB. After incubation at 37 °C for 2 h and cooling at 25 °C with 250 rpm shaking for 20 min, protein expression was induced with 1 mM of isopropyl-1-thio-D-galactopyranoside (IPTG). Following protein expression for 20 h, spheroplasts were prepared from 36 ml of culture broth for library screening.

***Library Screening*.** Glycosylated FcγRIIa-R131-GST (*6*) was labeled with Alexa488 using an Alexa488 labeling kit (Invitrogen). A competitive screen was used to isolate clones with high binding affinity for FcγRIIa over FcγRIIb in which spheroplasts were incubated with fluorescent FcγRIIa-R131-GST-Alexa488 with excess amounts of non-fluorescent FcγRIIb-GST present (concentration of FcγRIIa-R131-GST-Alexa488: concentration of non-fluorescent FcγRIIb-GST = 30 nM: 100 nM for the 1st round, 10 nM: 100 nM for the 2nd round, 10 nM : 100 nM for the 3rd round, 5 nM : 100 nM for the 4th round, and 5 nM : 200 nM for the 5th round of sorting). More than 4×10^8 spheroplasts were sorted in the first round of screening on a MoFlo flow cytometer (Dako Cytomation) equipped with a 488 nm argon laser for excitation. In each round, the top 3% of the population showing

the highest fluorescence was isolated and resorted immediately after the initial sorting. The heavy chain genes (VH-CH1-CH2-CH3) in the spheroplasts were amplified from the collected spheroplasts by PCR with two specific primers STJ#474 and STJ#67, ligated into *Sfi*I restriction enzyme digested pPelBFLAG-Fc, and transformed in electrocompetent *E. coli* Jude-1 cells. The resulting transformants were grown on chloramphenicol containing LB agar plates and prepared again as spheroplasts for the next round of sorting.

Protein Expression and Purification. AglycoT-Fc1001, AglycoT-Fc1002, AglycoT-Fc1003, AglycoT-Fc1004, GlycoT-G236A, AglycoT-N297D and the N297D variant of an anti-FcγRIIb 2B6 antibody (*3*) were produced by transient transfection of HEK293F cells (Invitrogen). pMAZ-IgL and pMAZ-IgH vectors for each of the variants were purified from overnight *E. coli* cultures by Midiprep (Qiagen). 293Fectin Transfection Reagent (Invitrogen) was used to transfect cells cultured in GIBCO FreeStyle™ 293 Expression Medium (Invitrogen) following the manufacturer's instructions. After 6 days, the cells were pelleted by centrifugation at 2,000 rpm for 10 min and the supernatant was recovered. 25x PBS was added to the supernatant to make a 1x final concentration and the solution was passed through a 0.22 µm filter. Protein A high capacity agarose resin (Thermo Scientific) was added to a polypropylene column and allowed to settle. The packed slurry was equilibrated with 1x PBS before addition of the buffered supernatant. The flow through was collected and passed twice more through the column. Unbound proteins were washed away with >10 CV (Column Volume) of 1x PBS. IgGs were eluted with 3 ml of 100 mM glycine-HCl (pH 2.7) and immediately neutralized with 1 ml of 1 M Tris (pH 8.0).

Samples were buffer-exchanged into 1x PBS using Amicon Ultra-4 (Millipore) spin columns with a 10 kDa cutoff. Purity of purified samples was assessed by 4-20% gradient SDS-PAGE gel (NuSep).

FcγRIIa-R131-GST, FcγRIIa-H131-GST, FcγRIIb-GST and FcγRIIIa-F158-GST were produced by transient transfection of HEK293F cells (Invitrogen) using the pMAZ-IgH expression vectors described. Receptors with GST fusion partners were purified by Glutathione Sepharose (GE Healthcare) affinity chromatography. 25x PBS was added to filtered supernatants to a 1x concentration and the mixture passed twice over the column. The column was washed with 100 ml of 1x PBS to remove nonspecifically bound protein. 4 ml of 1x PBS containing 10 mM reduced glutathione was used for elution into 10 kDa filter columns.

SPR Analysis. Surface plasmon resonance (SPR) was performed using a BIAcore 3000 instrument (GE Healthcare). Herceptin, AglycoT-Fc5-2a, AglycoT-Fc1001, AglycoT-Fc1002, AglycoT-Fc1003, and AglycoT-Fc1004 were individually immobilized on CM5 sensor chips by amine coupling as recommended by the manufacturer. Binding experiments were performed in HBS-EP buffer (10 mM HEPES pH 7.4, 150 mM NaCl, 3.4 mM EDTA, and 0.005% P20 surfactant)(GE Healthcare). Dimeric FcγRIIa-131R-GST, FcγRIIa-H131-GST, and FcγRIIb-GST receptors were injected in duplicate at a flow rate of 30 µl/min for 60 sec with a dissociation time of 5 min. The chip was regenerated after each run by sequential injection of 50 mM glycine, pH 4.0, 50 mM glycine, pH 9.5, and 3

M NaCl for 2 min each. For each run, a bovine serum albumin-coupled (BSA) surface was used to subtract non-specific receptor binding. Equilibrium dissociation constants (K_D) for monovalent receptor binding were determined by fitting a 2:1 bivalent analyte model ($A + 2B \rightleftharpoons AB + B \rightleftharpoons AB_2$) to the data using BIAevaluation 3.2 software (GE Healthcare) in accordance with earlier analyses (*8*). To determine binding to FcγRI, purified IgGs were immobilized on activated amine CM5 Biacore chips in 10 mM sodium acetate buffer (pH 5.0) and BSA in 10 mM sodium acetate (pH 5.0) was immobilized to a control lane on each chip for background receptor binding subtraction. 30 µl samples of purified FcγRI (R&D Systems) in HBS-EP running buffer were injected in duplicate and dissociation was monitored over a 5 min period. 10 mM glycine at pH 3.0 was used for chip regeneration between samples. The data were fit to a 1:1 Langmuir binding model as described earlier to obtain kinetic constants (*1*).

ELISAs. ELISA plates (Corning) were coated with 4 µg/ml of Her2 protein (Sino Biological) in 0.05M Na_2CO_3 (pH 9.5) overnight at 4 ^{o}C. The next day the plates were blocked at room temperature for 2 h with 2% milk in PBS containing 0.05% Tween (PBST) and washed four times in PBST at pH 7.4 before the addition of 4 µg/ml of antibody dissolved in PBS with 2% milk (PBSM). After 1 h of incubation, the plates were washed with PBST 4x and then 66 µl of FcγRIIIa-GST at 20 µg/ml added to the first well followed by 1:4 serial dilution. The plates were incubated at room temperature for 1 h, washed with PBS 4x and 50 µl PBSM was added containing goat anti-GST HRP (GE Healthcare)

1:5000 for 1 h. To develop the plates, the wells were washed 4x with PBST and 50 µl TMB substrate was added per well (Thermo Scientific). 50 µl of 1 M H_2SO_4 was used for neutralization and the final Abs_{450} was recorded.

HER2 Cell Surface Density. To qualitatively evaluate the density of HER2 receptors on the surface of SKBR-3 (ATCC), SKOV-3 (ATCC), and MDA-MB-453 (ATCC) cells, 10 µg/ml of Herceptin or IgG1 pooled from human serum (Sigma-Aldrich) as a control were incubated with 10^6 cells for 45 min on ice in 1 ml of Stain buffer (BD Biosciences). Subsequently, the Herceptin or IgG1 bound cells were washed with 1 ml of Stain buffer by centrifugation at 400 x g for 5 min, and labeled with 1:50 diluted donkey anti-human IgG (H+L) FITC-conjugate Fab (Jackson ImmunoResearch Laboratories) on ice for 45 min. The cells were washed twice more with 1 ml of Stain buffer following the centrifugation procedure above and cell fluorescence was analyzed by flow cytometry (BD FACSCalibur).

Preparation of Human Monocyte-derived Macrophages. PBMCs were isolated from fresh human pooled blood samples (Gulf Coast Regional Blood Center) by Histopaque (Sigma-Aldrich) gradient centrifugation. Briefly, 20 ml Histopaque was added to 50 ml conical tubes followed by 30 ml of blood gradually. The mixture was centrifuged for 15 min in a swinging bucket rotor without braking at 800 x g. PBMCs were aspirated from the sample and transferred to a fresh tube. The sample was washed twice with 50 ml

PBS containing 2% FBS (Mediatech) and 1 mM EDTA by centrifuging without braking at 120 x g for 10 min to remove platelets from the sample. $CD14^+$ monocytes were isolated by magnetic bead separation (Stemcell Technologies) according to the manufacturer's instructions. Cells were resuspended in RPMI (Invitrogen) containing 15% FBS and seeded at 1.5 x 10^6 cell per well in 96 well plates containing 3 ml of the same media supplemented with 50 ng/ml GM-CSF (R&D systems). The cells were grown at 37 °C in 5% CO_2 and at days 2 and 5 of culture and an additional 1 ml of media with fresh cytokine was added to each well. After 7 days, non-adherent cells were aspirated and the plate was washed with Dulbecco's PBS (Mediatech). 1 ml HyQTase (Thermo Scientific) solution was added for 15 min at 37 °C for the detachment of macrophages from the plate surface. Recovered cells were washed with 50 ml RPMI media and resuspended in RPMI containing 10% Human AB serum (Mediatech). Macrophage differentiation was confirmed by staining with 10 µg/ml anti-CD14-APC (Clone M5E2, Biolegend) and 10 µg/ml anti-CD11b-APC (Clone ICRF44, Biolegend).

Quantification of FcγRs on Macrophages. The anti-FcγRIIb antibody, 2B6-N297D (*3*) was transiently expressed and FITC labeled alongside an aglycosylated human IgG1 isotype control using a FITC conjugation kit (Invitrogen). Monocyte-derived macrophages were cultured as above and labeled separately with 20 µg/ml anti-FcγRI-FITC (Clone 10.1, Genetex), 10 µg/ml anti-FcγRIIa-FITC (Clone IV.3, Stemcell Technologies), 20 µg/ml anti-FcγRIII-FITC (Clone 3G8, ABcam), 1 µg/ml 2B6-N297D-FITC, 1 µg/ml human aglycosylated IgG1-FITC isotype control as well as FITC conjugated murine isotype control antibodies

for IgG1 (20 μg/ml Clone 15H6, Biolegend) and IgG2b (10 μg/ml Clone MG2b-57, Biolegend). Receptor counts were determined in a FACS assay by comparing the fluorescent values of antibody labeled macrophages to standard curves generated by bead standards that capture precisely known numbers of each of the labeling antibodies (Quantum Simply Cellular anti-mouse and anti-human, Bangs Laboratories).

Construction and Parameterization of Mathematical Model. A mathematical model was developed to better understand the interaction between Her2-expressing cells (SKOV-3 or MDA-MD-453) and macrophages. Within a "contact" area, Her2-bound IgG can bind to FcγRs, but this interaction is not possible outside of this region because of physical constraints imparted by the curvature of the two cells (Fig. 4*A*). This contact area was estimated to be 1/3 of the surface area of the smaller SKOV-3/MDA-MD-453 cells based on geometric considerations. A lower bound of 1/10 of the surface area has been calculated for a non-deforming bead (*9*), but the actual contact area is significantly higher because macrophages deform and spread around IgG-bound cells (*10, 11*). Model nomenclature and parameter values are provided in Table S4.

We considered three types of FcγRs on macrophages: FcγRIIa-H131, FcγRIIa-R131, and FcγRIIb. The number of FcγRIIa and FcγRIIb were experimentally quantified (Fig. S5*B*), and the FcγRIIa-H131 and FcγRIIa-R131 variants were assumed to exist in 50/50 proportions (*12*). FcγRs partitioned between the contact area and the free (non-contact) area with equilibrium constant K_{diff}:

$$\text{FcγRIIx}_{free} \xrightleftharpoons{K_{diff}} \text{FcγRIIx}_{contact}$$

where $K_{diff} = \frac{[\text{FcγRIIx}_{free}]}{[\text{FcγRIIx}_{contact}]} = \frac{[\text{Macrophage Surface Area - Contact Area}]}{[\text{Contact Area}]}$

and FcγRIIx = FcγRII-H131, FcγRII-R131 or FcγRIIb

All Her2 receptors on SKOV-3 and MDA-MD-453 cells were considered to be evenly distributed and receptor numbers were calculated from experimental quantification of relative expression levels (Fig. S5*A*) and total absolute values from literature (*13, 14*). The effective concentration of cell-bound IgG ($[L_0]$) was calculated in an "effective contact volume," defined as the product of contact_area and cell_gap. These cell-bound IgGs were free to interact with FcγRIIx $_{contact}$ with ligand depletion:

$$L + \text{FcγRIIx}_{contact} \xrightleftharpoons{K_{D\_x}} \text{FcγRIIx}_{cell\text{-}bound}$$

where $K_{D\_x} = K_{D\_IIa\text{-}H131}$, $K_{D\_IIa\text{-}R131}$, or K_{D_IIb} from SPR data for different Fc variants (Table S3).

To mimic conditions in our *in vitro* experiments, as well as in normal physiology, 10 μM serum IgG ($[IgG]_s$) was included in the system. Serum IgG was assumed to be in excess and could bind FcγRIIs anywhere on the macrophage surface without ligand depletion:

$$IgG_S + \text{FcγRIIx}_{free} \xrightleftharpoons{K_{D\_x\_IgG}} \text{FcγRIIx}_{free\ I\ bound}$$

$$IgG_S + \text{FcγRIIx}_{contact} \xrightleftharpoons{K_{D\_x\_IgG}} \text{FcγRIIx}_{contact\ I\ bound}$$

where $K_{D\_x\_IgG} = K_{D\_IIa\_IgG}$ or $K_{D\_IIb\_IgG}$.

Since receptor crosslinking leads to cell activation or inhibition, we assumed that dimers represent the minimal signaling unit (and serve as proxies for any higher-order receptor

clusters). Any IgG-bound FcγRIIs were allowed to dimerize with equilibrium dissociation constant K_{cross}. K_{cross} was chosen to be 2500 #/μm^2, which maximizes the difference in the number of crosslinked receptors with and without MDA-MB-453 cells (chosen for this signal optimization since they express fewer Her2 molecules than SKOV-3 cells and therefore have lower signals). All possible combinations of dimers were allowed between the three FcγRII subunits with the same crosslinking constant, whether occupied by serum IgG or Her2-bound IgG. However, geometric constraints limited receptors in the contact area to only crosslink with those in the contact area, while receptors outside of the contact area could only crosslink with those outside:

$$\text{FcγRIIx}_{\text{cell-bound}} + \text{FcγRIIx}_{\text{cell-bound}} \underset{}{\overset{K_{cross}}{\rightleftharpoons}} \text{FcγRIIx} - \text{FcγRIIx}$$

$$\text{FcγRIIx}_{\text{contact I bound}} + \text{FcγRIIx}_{\text{contact I bound}} \overset{K_{cross}}{\rightleftharpoons} \text{FcγRIIx} - \text{FcγRIIx}$$

$$\text{FcγRIIx}_{\text{free I bound}} + \text{FcγRIIx}_{\text{free I bound}} \overset{K_{cross}}{\rightleftharpoons} \text{FcγRIIx} - \text{FcγRIIx}$$

No discrimination was made between crosslinked receptors in and out of the contact area because all of them could lead to an activating or inhibitory signal. However, local concentration effects made the density of dimers (and potentially higher-order clusters) much higher in the contact area.

The diffusion, binding, and crosslinking reactions above yield the following system of equations (x = IIa-H131, IIa-R131, or IIb):

$$\left[\text{FcγRIIx}\right]_{\text{free}} = K_{\text{diff}} \left[\text{FcγRIIx}\right]_{\text{contact}} \qquad \text{(E1, E2, E3)}$$

$$\left(\frac{\left[L_0\right]_{SK/MD} - \left[FcγRIIx\right]_{cell\text{-}bound}}{\left(N_{AV} \times cell\_gap\right)}\right) \times \left[FcγRIIx\right]_{contact} = K_{D\_x}\left[FcγRIIx\right]_{cell\text{-}bound} \quad \text{(E4, E5, E6)}$$

$$\left[IgG\right]_S\left[FcγRIIx\right]_{free} = K_{D\_x\_IgG}\left[FcγRIIx\right]_{free\ I\ bound} \quad \text{(E7, E8, E9)}$$

$$\left[IgG\right]_S\left[FcγRIIx\right]_{contact} = K_{D\_x\_IgG}\left[FcγRIIx\right]_{contact\ I\ bound} \quad \text{(E10, E11, E12)}$$

$$\left[FcγRIIx\right]_{cell\text{-}bound}\left[FcγRIIx\right]_{cell\text{-}bound} = K_{cross}\left[FcγRIIx{:}FcγRIIx\right] \quad \text{(E13 to E18)}$$

$$\left[FcγRIIx\right]_{contact\ I\ bound}\left[FcγRIIx\right]_{cell\text{-}bound} = K_{cross}\left[FcγRIIx{:}FcγRIIx\right] \quad \text{(E19 to E27)}$$

$$\left[FcγRIIx\right]_{free\ I\ bound}\left[FcγRIIx\right]_{free\ I\ bound} = K_{cross}\left[FcγRIIx{:}FcγRIIx\right] \quad \text{(E28 to E33)}$$

where [FcγRIIx] is in #/μm^2. Conservation of mass gives:

$$\text{all}\left[FcγRIIx\right]\text{in free area} \times \left(\text{macrophage total surface area} - \text{contact\_area}\right)$$
$$+\,\text{all}\left[FcγRIIx\right]\text{in contact area} \times \text{contact\_area} = \text{Mac\_IIx}$$

(E34, E35, E36)

This system of equations was solved in Matlab using *fsolve* to obtain the 36 unknowns. Finally, the resulting distribution of FcγRII dimers was correlated to the experimental output of ADCP. The relative contribution of activating/inhibiting homodimers to this cellular response is not known and, although there is evidence that heterodimers (FcγRIIa crosslinked with FcγRIIb) do form (*15*), it is not known whether they activate or inhibit. Therefore, we did not assign any *a priori* functions or signaling weights to these species, but rather allowed their contributions to be determined by the model by assigning an "intrinsic signaling potency" to each subunit. The signaling potency for FcγRIIb was fixed at -1 (negative for inhibitory) and the signaling potencies for FcγRIIa-

H131 and FcγRIIa-R131 were allowed to vary freely. We then assumed that the signaling potency of any given dimer was equal to the sum of potency of individual receptors. The overall response was calculated from:

$$\text{phagocytosis} \propto \sum\left(\text{FcγRIIx : FcγRIIx} \times \text{signaling potency of the respective dimer}\right)$$

The level of phagocytosis was then compared to experimental data for only two Fc variants to obtain the intrinsic signaling potencies for FcγRIIa-H131 and FcγRIIa-R131. Fitted potency values are presented in Table S5.

References

1. Jung, S. T., Reddy, S., Kang, T., Borrok, M., Sandlie, I., Tucker, P., and Georgiou, G. (2010) Aglycosylated IgG variants expressed in bacteria that selectively bind FcγRI potentiate tumor cell killing by monocyte-dendritic cells, *Proc Natl Acad Sci USA 107*, 604-609.
2. Jung, S. T., Jeong, K. J., Iverson, B. L., and Georgiou, G. (2007) Binding and enrichment of Escherichia coli spheroplasts expressing inner membrane tethered scFv antibodies on surface immobilized antigens, *Biotechnol Bioeng 98*, 39-47.
3. Veri, M. C., Gorlatov, S., Li, H., Burke, S., Johnson, S., Stavenhagen, J., Stein, K. E., Bonvini, E., and Koenig, S. (2007) Monoclonal antibodies capable of discriminating the human inhibitory Fcγ-receptor IIB (CD32B) from the activating Fcγ-receptor IIA (CD32A): biochemical, biological and functional characterization, *Immunology 121*, 392-404.
4. Bryksin, A. V., and Matsumura, I. (2010) Overlap extension PCR cloning: a simple and reliable way to create recombinant plasmids, *Biotechniques 48*, 463-465.
5. Kawarasaki, Y., Griswold, K. E., Stevenson, J. D., Selzer, T., Benkovic, S. J., Iverson, B. L., and Georgiou, G. (2003) Enhanced crossover SCRATCHY: construction and high-throughput screening of a combinatorial library containing multiple non-homologous crossovers, *Nucleic Acids Res 31*, e126-e126.
6. Berntzen, G., Lunde, E., Flobakk, M., Andersen, J. T., Lauvrak, V., and Sandlie, I. (2005) Prolonged and increased expression of soluble Fc receptors, IgG and a TCR-Ig fusion protein by transiently transfected adherent 293E cells, *J Immunol Methods 298*, 93-104.
7. Fromant, M., Blanquet, S., and Plateau, P. (1995) Direct random mutagenesis of gene-sized DNA fragments using polymerase chain reaction, *Anal Biochem 224*, 347-353.
8. Pabbisetty, K. B., Yue, X., Li, C., Himanen, J. P., Zhou, R., Nikolov, D. B., and Hu, L. (2007) Kinetic analysis of the binding of monomeric and dimeric ephrins to Eph receptors: Correlation to function in a growth cone collapse assay, *Protein Sci 16*, 355-361.
9. Kuo, S. C., and Lauffenburger, D. A. (1993) Relationship between receptor/ligand binding affinity and adhesion strength, *Biophys J 65*, 2191-2200.
10. Heiple, J. M., Wright, S. D., Allen, N. S., and Silverstein, S. C. (1990) Macrophages form circular zones of very close apposition to lgG-Coated surfaces, *Cell Motil Cytoskel 15*, 260-270.
11. Tolentino, T. P., Wu, J., Zarnitsyna, V. I., Fang, Y., Dustin, M. L., and Zhu, C. (2008) Measuring diffusion and binding kinetics by contact area FRAP, *Biophys J 95*, 920-930.
12. Reilly, A., Norris, C., Surrey, S., Bruchak, F., Rappaport, E., Schwartz, E., and McKenzie, S. (1994) Genetic diversity in human Fc receptor II for immunoglobulin G: Fc gamma receptor IIA ligand-binding polymorphism, *Clin Vaccine Immunol 1*, 640-644.
13. Costantini, D. L., Bateman, K., McLarty, K., Vallis, K. A., and Reilly, R. M. (2008) Trastuzumab-resistant breast cancer cells remain sensitive to the auger electron–emitting radiotherapeutic agent ^{111}In-NLS-trastuzumab and are radiosensitized by methotrexate, *J Nucl Med 49*, 1498-1505.
14. Xu, F., Yu, Y., Bae, D., Zhao, X. G., Slade, S., Boyer, C., Bast, R., and Zalutsky, M. (1997) Radioiodinated antibody targeting of the HER-2/*neu* oncoprotein, *Nucl Med Biol 24*, 451-459.
15. Smith, K. G. C., and Clatworthy, M. R. (2010) FcgammaRIIB in autoimmunity and infection: evolutionary and therapeutic implications, *Nat Rev Immunol 10*, 328-343.
16. Zhang, X., Chen, J., Zheng, Y., Gao, X., Kang, Y., Liu, J., Cheng, M., Sun, H., and Xu, C.

(2009) Follicle-stimulating hormone peptide can facilitate paclitaxel nanoparticles to target ovarian carcinoma *in vivo*, *Cancer Res 69*, 6506-6514.

17. Rhodes, A., Jasani, B., Anderson, E., Dodson, A. R., and Balaton, A. J. (2002) Evaluation of HER-2/neu immunohistochemical assay sensitivity and scoring on formalin-fixed and paraffin-processed cell lines and breast tumors, *Am J Clin Pathol 118*, 408-417.
18. Krombach, F., Münzing, S., Allmeling, A. M., Gerlach, J. T., Behr, J., and Dörger, M. (1997) Cell size of alveolar macrophages: an interspecies comparison, *Environ Health Persp 105*, 1261-1263.
19. Pease III, L. F., Elliott, J. T., Tsai, D. H., Zachariah, M. R., and Tarlov, M. J. (2008) Determination of protein aggregation with differential mobility analysis: application to IgG antibody, *Biotechnol Bioeng 101*, 1214-1222.
20. Sondermann, P., Huber, R., and Jacob, U. (1999) Crystal structure of the soluble form of the human Fcγ-receptor IIb: a new member of the immunoglobulin superfamily at 1.7 Å resolution, *EMBO J 18*, 1095-1103.
21. Maenaka, K., van der Merwe, P. A., Stuart, D. I., Jones, E. Y., and Sondermann, P. (2001) The human low affinity Fcγ receptors IIa, IIb, and III bind IgG with fast kinetics and distinct thermodynamic properties, *J Biol Chem 276*, 44898-44904.

Table S1. Plasmids used in this work.

Plasmids	Relevant characteristics	Reference or Source
pPelBFLAG	Cm^r, *lac* promoter, *tetA* gene, *skp* gene, C-terminal FLAG tag	(*1*)
pPelBFLAG-Fc	*IgG1-Fc* gene in pPelBFLAG	(*1*)
pTrc99A-DsbA-Fc-FLAG	*dsbA fused IgG1-Fc* gene, C-terminal FLAG tag in pTrc99A	(*1*)
pTrc99A-DsbA-Fc2a-FLAG	*dsbA fused IgG1-Fc2a* gene, C-terminal FLAG tag in pTrc99A	This study
pSTJ4-AglycoT	Trastuzumab IgG1 gene in pMAZ360	(*1*)
pSTJ4-AglycoT-Fc5	Trastuzumab IgG1-Fc5 gene in pMAZ360	(*1*)
pSTJ4-AglycoT-Fc2a	Trastuzumab IgG1-Fc2a gene in pMAZ360	This study
pSTJ4-AglycoT-Fc5-2a	Trastuzumab IgG1-Fc5-2a gene in pMAZ360	This study
pPelB-AglycoT(H)-FLAG	Trastuzumab IgG1 heavy chain gene in pPelBFLAG	This study
pPelB-AglycoT(H)-Fc5-FLAG	*IgG1-Fc5 heavy chain* gene in pPelB-AglycoT(H)-FLAG	This study
pPelB-AglycoT(H)-Fc2a-FLAG	*IgG1-Fc2a heavy chain* gene in pPelB- AglycoT(H)-FLAG	This study
pPelB-AglycoT(H)-Fc5-2a-FLAG	*IgG1-Fc5-2a heavy chain* gene in pPelB- AglycoT(H)-FLAG	This study
pPelB-AglycoT(H)-Fc1001-FLAG	*IgG1-Fc1001 heavy chain* gene in pPelB- AglycoT(H)-FLAG	This study
pPelB-AglycoT(H)-Fc1004-FLAG	*IgG1-Fc1004 heavy chain* gene in pPelB- AglycoT(H)-FLAG	This study
pPelB-AglycoT(H)-FcG236A-FLAG	*IgG1-FcG236A heavy chain* gene in pPelB- AglycoT(H)-FLAG	This study
pMoPac1-FLAG-M18	NlpA fused *M18 scFv gene*, C-terminal FLAG tag in pMoPac1	(*2*)
pBAD30-KmR	Km^r, BAD promoter	(*2*)
pBADNlpAHis-M18	NlpA fused *M18 scFv*, C-terminal polyhistidine tag in pBAD30	This study
pBADNlpA-VL-Cκ-His	NlpA fused *trastuzumab VL-Cκ domain*, C-terminal polyhistidine tag and c-myc tag in pBAD30-KmR	This study
pBADPelB-VL-Cκ-His	PelB fused *trastuzumab VL-Cκ domain*, C-terminal polyhistidine tag and c-myc tag in pBAD30-KmR	This study
pBAD-AglycoT(L)-His	PelB fused trastuzumab VL-Cκ domain followed by Nlp A fused trastuzumab VL-Cκ-His in pBAD30-KmR for dicistronic expression	This study
pMAZ-IgH-GlycoT	Trastuzumab IgG1 heavy chain gene in pMAZ-IgH-H23	(*1*)
pMAZ-IgH-GlycoT-Fc1001	IgG1-Fc1001 heavy chain gene in pMAZ-IgH-GlycoT	This study
pMAZ-IgH-GlycoT-Fc1002	IgG1-Fc1002 heavy chain gene in pMAZ-IgH-GlycoT	This study
pMAZ-IgH-GlycoT-Fc1003	IgG1-Fc1003 heavy chain gene in pMAZ-IgH-GlycoT	This study

pMAZ-IgH-GlycoT-Fc1004	IgG1-Fc1004 heavy chain gene in pMAZ-IgH-GlycoT	This study
pMAZ-IgH-GlycoT-FcG236A	IgG1-FcG236A heavy chain gene in pMAZ-IgH-GlycoT	This study
pMAZ-IgH-GlycoT-FcN297D	IgG1-FcN297D heavy chain gene in pMAZ-IgH-GlycoT	This study
pMAZ-IgH-2B6-N297D	2B6-N297D IgG1 heavy chain gene in pMAZ-IgH-GlycoT	This study
pMAZ-IgL-GlycoT	Trastuzumab IgG1 light gene in pMAZ-IgH-H23	(*1*)
pMAZ-IgL-2B6-N297D	2B6-N297D IgG1 light chain gene in pMAZ-IgH-GlycoT	(*1*)
pDNR-LIB-FcγRIIa	*FcγRIIa*$_{H131}$ gene in pMAZ-IgH-GlycoT	ATCC
pCMV-SPORT6-FcrRIIIa	*FcγRIIIa*$_{V158}$ gene in pMAZ-IgH-GlycoT	ATCC
pMAZ-FcγRI-GST	*FcγRI-GST* gene in pMAZ-IgH-GlycoT	This study
pMAZ-FcγRIIa$_{R131}$-GST	*FcγRIIa*$_{R131}$*-GST* gene in pMAZ-IgH-GlycoT	This study
pcDNA3(oriP)-FcγRI	*FcγRI* gene with C-Terminal GST fusion for mammalian expression	(*6*)
pMAZ-FcγRIIa$_{H131}$-GST	*FcγRIIa*$_{H131}$*-GST* gene in pMAZ-IgH-GlycoT	This study
pMAZ-FcγRIIIa$_{V158}$-GST	*FcγRIIIa*$_{V158}$*-GST* gene in pMAZ-IgH-GlycoT	This study
pMAZ-FcγRIIIa$_{F158}$-GST	*FcγRIIIa*$_{F158}$*-GST* gene in pMAZ-IgH-GlycoT	This study

Table S2. Primers used in this study (Underlining indicates the restriction enzyme sites).

Primer Name	Primer nucleotide sequence (5' → 3')
STJ#16	TTGTGAGCGGATAACAATTTC
STJ#67	AATTCGGCCCCCGAGGCCCCTTTACCCGGGGACAGGGAGAGGCTCTTCTGCGTG
STJ#70	CTACCTGACGCTTTTTATCGC
STJ#76	CGCAGCGAGGCCCAGCCGGCCATGGCGGGCATGCGGACTGAAGATCTC
STJ#82	CGCAATTCGGCCCCCGAGGCCCCTTGGTACCCAGGTGGAAAGAATG
STJ#147	GGCAAATTCTGTTTTATCAGACCGCTTCTG
STJ#220	CAATTTTGTCAGCCGCCTGAGCAGAAG
STJ#290	TTTTAGGGTTTTAGGGGTCGACAAGAAAGTTGAGCCCAAATCTTGTGACAAAACTCACACATGCCC ACCG
STJ#290	TTTTAGGGGTCGACAAGAAAGTTGAGCCCAAATCTTGTGACAAAACTCACACATGCCCACCG
STJ#291	GGCCACCGGATATCTTATTATTTACCCGGGGACAGGGAGAGG
STJ#332	GGGAATTCTAGACTATTAGCACTCTCCCCTGTTGAAGCTCTTTG
STJ#340	TTTAAGGGAAGCTTCTATTAGCACTCTCCCCTGTTGAAGCTCTTTG
STJ#422	CTAGGGAGCCGCGGGAGGAGCAGTACAACGGCGCGTACCGTGTGGTCAGCGTCCTC
STJ#474	CGCAGCGAGGCCCAGCCGGCCATGGCGGAGGTTCAATTAGTGGAATCTG
STJ#475	CGCAGCGAGGCCCAGCCGGCCATGGCGGATATTCAAATGACCCAAAGCCCG
STJ#476	CGCAATTCGGCCCCCGAGGCCCCGCACTCTCCCCTGTTGAAGCTCTTTG
STJ#490	CTAGGGAGCCGCGGGAGGAGCAGTACAACGGCGCGTACCGTGTGGTCAGTGTCCTC
STJ#498	TTTTAGGGTCTAGATCATTTACCCGGGGACAGGGAGAGG
WK#56	TCCACAGGCGCGCACTCCCAAGTGGACACCACAAAGGCAGTG
WK#57	GGCTGATCAGCGAGCTTCTAGATCAGGATCTTTTTGGAGGATGGTCGC
WK#91	CTCCACAGGCGCGCACTCCGGCATGCGGACTGAAGATCTCCC
WK#92	CCACGCGGAACCAGCTCGAGTTGGTACCCAGGTGGAAAGAATGATG
WK#94	GTTCACAGTCTCTGAAGACACATTTTTACTCCCGAAAAGCCCCCTGCAGAAG
WK#100	CTCTCCACAGGCGCGCACTCCCAAGCTGCTCCCCCAAAGGCTGT
WK#101	CCACGCGGAACCAGCTCGAGCCCCATTGGTGAAGAGCTGCCC
WK#116	GCTTGTGGGATGGAGAAGGTGGGATCCAACCGGGAGAATTTCTGGG
WK#158	CTCCACAGGCGCGCACTCCGAAATTGTGCTGACTCAGTCTCCAGACTTTC
WK#159	GGTGACTTTCTCCTTTGGTGTCACGCTCTGAAAGTCTGGAGACTGAGTCAGCACAATTTC
WK#160	AGAGCGTGACACCAAAGGAGAAAGTCACCATCACCTGCAGGACCAGTCAGAGC
WK#161	GCTGGTACCAATGTATGTTTGTGCCAATGCTCTGACTGGTCCTGCAGGTGAT
WK#162	ATTGGCACAAACATACATTGGTACCAGCAGAAACCAGATCAGTCTCCAAAGCTCC
WK#163	GACTCCAGAGATAGACTCAGAAACATACTTGATGAGGAGCTTTGGAGACTGATCTGGTTTCT
WK#164	TCATCAAGTATGTTTCTGAGTCTATCTCTGGAGTCCCATCGAGGTTCAGTGGCAGTGG
WK#165	GGTGAGGGTGAAATCTGTCCCTGATCCACTGCCACTGAACCTCGATGG
WK#167	ATCAGGGACAGATTTCACCCTCACCATCAATAGCCTGGAAGCTGAAGATGCTG
WK#168	GCCAGGTATTACTTTGTTGACAGTAATACGTTGCAGCATCTTCAGCTTCCAGGCTATTGAT
WK#169	CAACGTATTACTGTCAACAAAGTAATACCTGGCCGTTCACGTTCGGCGGAGG
WK#170	CGATGGGCCCTTGGTGCTAGCTTTGATCTCCACCTTGGTCCCTCCGCCGAACGTGAACG
WK#171	GCGGCCGCCGTGCGTTTGATCTCCACCTTGGTC
WK#172	CTCCACAGGCGCGCACTCC
WK#173	CTCCACAGGCGCGCACTCCCAGGTTCAGCTGGTGCAGTCTGG
WK#174	CCCCAGGCTTCTTCACCTCAGCTCCAGACTGCACCAGCTGAACCTG
WK#175	AGCTGAGGTGAAGAAGCCTGGGGCCTCAGTGAAGGTCTCCTGCAAGG
WK#176	GTATCCAGTAGTTGGTAAAGGTGTAACCAGAAGCCTTGCAGGAGACCTTCACTGAGG
WK#177	CTTCTGGTTACACCTTTACCAACTACTGGATACACTGGGTGCGACAGGCGCC

WK#178	CCATCCACTCAAGCCCTTGTCCAGGCGCCTGTCGCACCCAGT
WK#179	TGGACAAGGGCTTGAGTGGATGGGAGTGATTGATCCTTCTGATACTTATCCAAATTAC
WK#180	CATGGTGACTCTGCCCTTGAACTTTTTATTGTAATTTGGATAAGTATCAGAAGGATCAATCACTC
WK#181	AATAAAAAGTTCAAGGGCAGAGTCACCATGACCACAGACACATCCACGAGCACAG
WK#182	CTCAGGCTCCTCAGCTCCATGTAGGCTGTGCTCGTGGATGTGTCTGTGGT
WK#183	CCTACATGGAGCTGAGGAGCCTGAGATCTGACGACACGGCCGTGTATTAC
WK#184	CGGAATCACCGTTTCTCGCACAGTAATACACGGCCGTGTCGTCAGAT
WK#185	TGTGCGAGAAACGGTGATTCCGATTATTACTCTGGTATGGACTACTGGGGGC
WK#186	GAGACGGTGACCGTGGTCCCTTGCCCCCAGTAGTCCATACCAGAGTAATAAT
WK#187	AAGGGACCACGGTCACCGTCTCCTCAGCTAGCACCAAGGGCCCATCG

Table S3. Kinetic on and off rates for trastuzumab Fc variant binding to FcγRs as determined by SPR analysis.

Variant	FcγRI			FcγRIIa-H131		
	K_{on} (M^{-1} s^{-1})	k_{off} (s^{-1})	K_D (nM)	k_{on} (M^{-1} s^{-1})	k_{off} (s^{-1})	K_D (μM)
Herceptin	1.8×10^5	2.7×10^{-4}	1.5[#]	7.2×10^5	8.5×10^{-2}	0.12
AglycoT-Fc5-2a	1.5×10^5	2.3×10^{-3}	16	3.1×10^5	1.2×10^{-1}	0.37
AglycoT-Fc1001	4.3×10^5	3.3×10^{-2}	77	2.6×10^5	5.4×10^{-2}	0.20
AglycoT-Fc1002	N/A	N/A	N/A	1.5×10^5	2.8×10^{-2}	0.19
AglycoT-Fc1003	N/A	N/A	N/A	3.3×10^5	5.9×10^{-2}	0.18
AglycoT-Fc1004	4.0×10^5	2.6×10^{-2}	64	5.3×10^5	1.1×10^{-2}	0.021

Variant	FcγRIIa-R131			FcγRIIb		
	k_{on} (M^{-1} s^{-1})	k_{off} (s^{-1})	K_D (μM)	k_{off} (s^{-1})	k_{on} (M^{-1} s^{-1})	K_D (μM)
Herceptin	1.2×10^5	3.7×10^{-2}	0.31	3.7×10^{-2}	1.2×10^5	1.3
AglycoT-Fc5-2a	1.3×10^5	3.6×10^{-2}	0.27	3.6×10^{-2}	1.3×10^5	1.6
AglycoT-Fc1001	2.6×10^5	3.9×10^{-3}	0.015	3.9×10^{-3}	2.6×10^5	0.47
AglycoT-Fc1002	1.8×10^5	4.0×10^{-2}	0.22	4.0×10^{-2}	1.8×10^5	1.9
AglycoT-Fc1003	2.6×10^5	3.2×10^{-2}	0.12	3.2×10^{-2}	2.6×10^5	1
AglycoT-Fc1004	3.2×10^5	6.2×10^{-4}	0.0019	6.2×10^{-4}	3.2×10^5	0.2

[#]Affinity reported in previous study (*1*), using the same method.

Table S4. Parameters used to generate FcγRIIa/b activation model

Parameter	Description	Value	Reference or Source
Physical parameters			
SK_dia	Diameter of SKOV-3 cell	10 µm	(*16*)
MD_dia	Diameter of MDA-MB-453 cell	10 µm	(*16, 17*)
Mac_dia	Diameter of macrophage	21 µm	(*18*)
Cell_gap	Gap distance between SKOV-3/MDA-MB-453 cell and macrophage	12 nm	(*19, 20*)
Contact_area	Contact area of FcγRII receptors on macrophage	104.7 μm^2	(*9-11*)
Expression level parameters			
SK_HER2	HER2 expression level on SKOV-3	7.36×10^5	(*13, 14*)
MD_HER2	HER2 expression level on MDA-MB-453	4.00×10^5	(*13, 14*)
Mac_IIaH	Number of FcγRIIa-H131 on macrophage	171271	This work
Mac_IIaR	Number of FcγRIIa-R131 on macrophage	171271	This work
Mac_Iib	Number of FcγRIIb on macrophage	291150	This work
$[IgG]_s$	Free serum IgG concentration	10 µM	This work
$[L_0]_{SK}$	SKOV-3 Her2-bound IgG effective concentration	324.2 µM	This work
$[L_0]_{MD}$	MDA-MB-453 Her2-bound IgG effective concentration	176.2 µM	This work
Affinity parameters			
K_{diff}	Equilibrium constant for partitioning of FcγRII receptors in/out of the contact area on macrophage	16.64	This work
K_{cross}	Equilibrium dissociation constant for the crosslinking of FcγRII receptors	2500 /μm^2	This work
$K_{D\_IIa\_IgG}$	Equilibrium dissociation constant between serum IgG and FcγRIIa-H131/FcγRIIa-R131	0.72 µM	(*21*)
$K_{D\_IIb\_IgG}$	Equilibrium dissociation constant between serum IgG a nd FcγRIIb	2.4 µM	(*21*)
$K_{D\_IIa\text{-}H131}$	Equilibrium dissociation constant between Fc variants and FcγRIIa-H131	(Table S3)	This work
$K_{D\_IIa\text{-}R131}$	Equilibrium dissociation constant between Fc variants and FcγRIIa-R131	(Table S3)	This work
K_{D_IIb}	Equilibrium dissociation constant between Fc variants and FcγRIIb	(Table S3)	This work

Table S5. Intrinsic signaling potencies of FcγRIIa-H131, FcγRIIa-R131, and FcγRIIb.

ADCP data considered	Intrinsic signaling potency		
	FcγRIIa-H131	**FcγRIIa-R131**	**FcγRIIb***
Fitting Herceptin and AglycoT-Fc1001 only	2.8	0.4	-1
Fitting Herceptin and AglycoT-Fc1004 only	2.0	0.3	-1
Fitting AglycoT-Fc1001 and AglycoT-Fc1004 only	11.3	0.1	-1

* The signaling potency of FcγRIIb was always held fixed at -1, since the goal of each fit was to determine the *relative* potencies among the three receptor subunits.

Figure S1. *E. coli* bacterial expression system for the display of full length IgGs. (*A*) Expression cassettes for the display of covalently anchored full length IgGs. (*B* and *C*) Fluorescence histograms of spheroplasts expressing full length AgylcoT-Fc5 (E382V/M428I) binding to 30 nM FcγRI-FITC (*B*) or AgylcoT-2a (S298G/T299A) binding to 30 nM FcγRIIa-GST followed by 1:200 diluted goat anti-GST-FITC (*C*). (*D*) AglycoT-Fc5-2a shows high affinity binding for 30 nM FcγRI, FcγRIIa, and FcγRIIb.

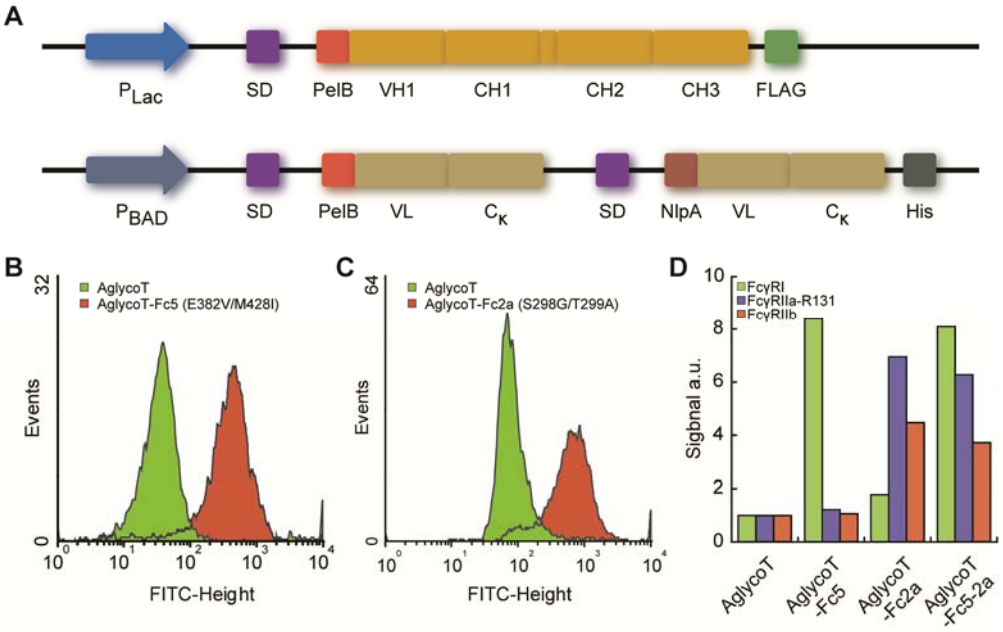

Figure S2. Sequences and corresponding FACS signals for isolated Fc variants.

```
                          Hinge                                CH2
                          220       230       240       250       260       270       280       290
FcWT      (75.76)         [---------]-------------------------------------------------------------ST
Fc5-2a   (135.76)         [DKTHTCPPC]PAPELLGGPSVFLFPPKPKDTLMISRTPEVTCVVVDVSHEDPEVKFNWYVDGVEVHNAKTKPREEQYNGA
Fc1001   (408.55)         [---------]-------------------------------------P-------------------------K-----
Fc1002   (303.82)         [---------]-------------------------------------------------------------------
Fc1003   (276.75)         [---------]-------------------------------------------------------------------
Fc1004   (256.43)         [---------]-------------------------------------------------------------------

                                                                                  CH3
                          300       310       320       330       340       350       360       370
FcWT      (75.76)         ----------------------------------------[-----------------------------------
Fc5-2a   (135.76)         YRVVSVLTVLHQDWLNGKEYKCKVSNKALPAPIEKTISKAK[GQPREPQVYTLPPSRDELTKNQVSLTCLVKGFYPSDIAV
Fc1001   (408.55)         ----------------------------------------[-----------------------------------
Fc1002   (303.82)         ---------------D------------------------[-----------------------------------
Fc1003   (276.75)         ----------------------------------------[-----------------------------------
Fc1004   (256.43)         ----------------------------------------[-----------------------------------

                                                      CH3
                          380       390       400       410       420       430       440
FcWT      (75.76)         --E---------------------------------------------M------------------]
Fc5-2a   (135.76)         EWVSNGQPENNYKTTPPVLDSDGSFFLYSKLTVDKSRWQQGNVFSCSVIHEALHNHYTQKSLSLSPGK]
Fc1001   (408.55)         ------------------------------------------------L------------------]
Fc1002   (303.82)         ------------------------------------------------L------------------]
Fc1003   (276.75)         ------------E----M-----------------------------L------------------]
Fc1004   (256.43)         ----------D-----------------------------------L------------------]
```

1) FACS mean values are indicated in the parenthesis

Figure S3. Characterization of isolated aglycosylated Fc variants. (A) Fluorescent histogram of variant binding to 30 nM FcγRIIa as detected by secondary goat anti-GST-FITC diluted at 1:200 from a 1 mg/ml stock. (B) SDS-PAGE showing full length trastuzumab Fc variants purified from HEK293F cells; M: molecular weight ladder, 1: AglycoT-Fc1001, 2: AglycoT-Fc1002, 3: AglycoT-Fc1003, and 4: AglycoT-Fc1004. (C and D) ELISA analysis of isolated aglycosylated Fc variants and Herceptin for (C) binding to FcγRIIIa, and (D) binding to FcRn at pH 6.0 and 7.4.

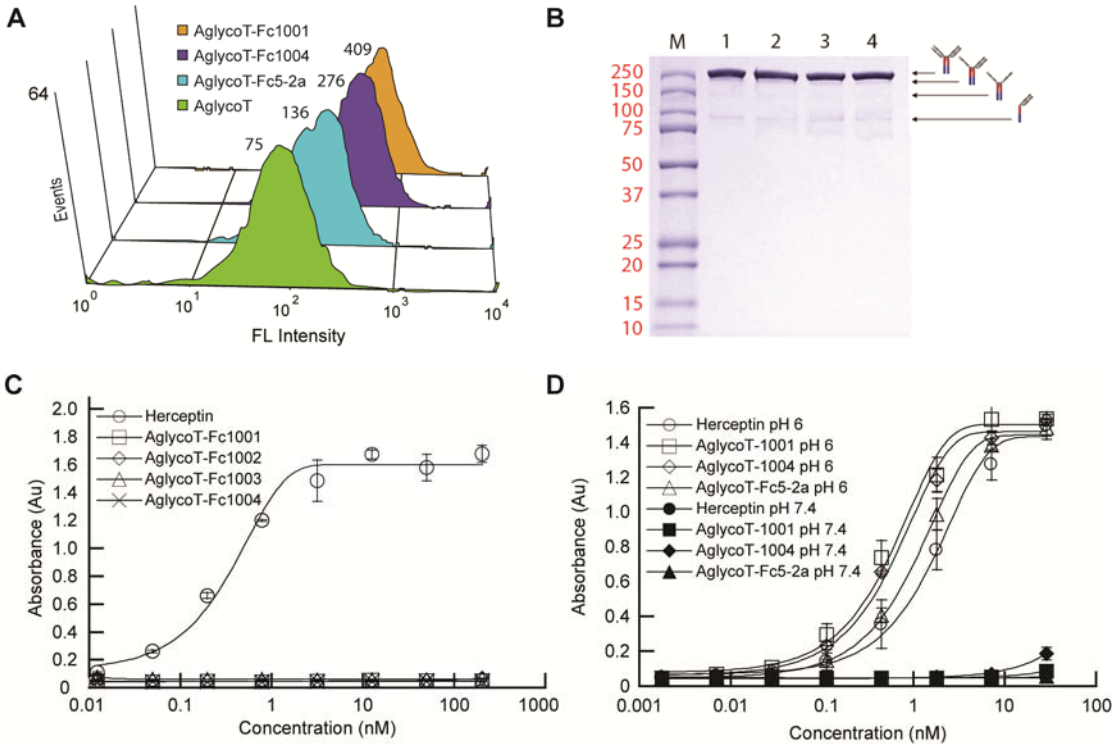

Figure S4. Biacore sensorgrams for FcγRIIa-R131-GST, FcγRIIa-H131-GST and FcγRIIb-GST binding to aglycosylated mutants. Antibody variants were immobilized on CM5 chips and soluble dimeric FcγRs used as analytes. A bivalent kinetic model was used to fit a minimum of four concentrations in duplicate for each variant.

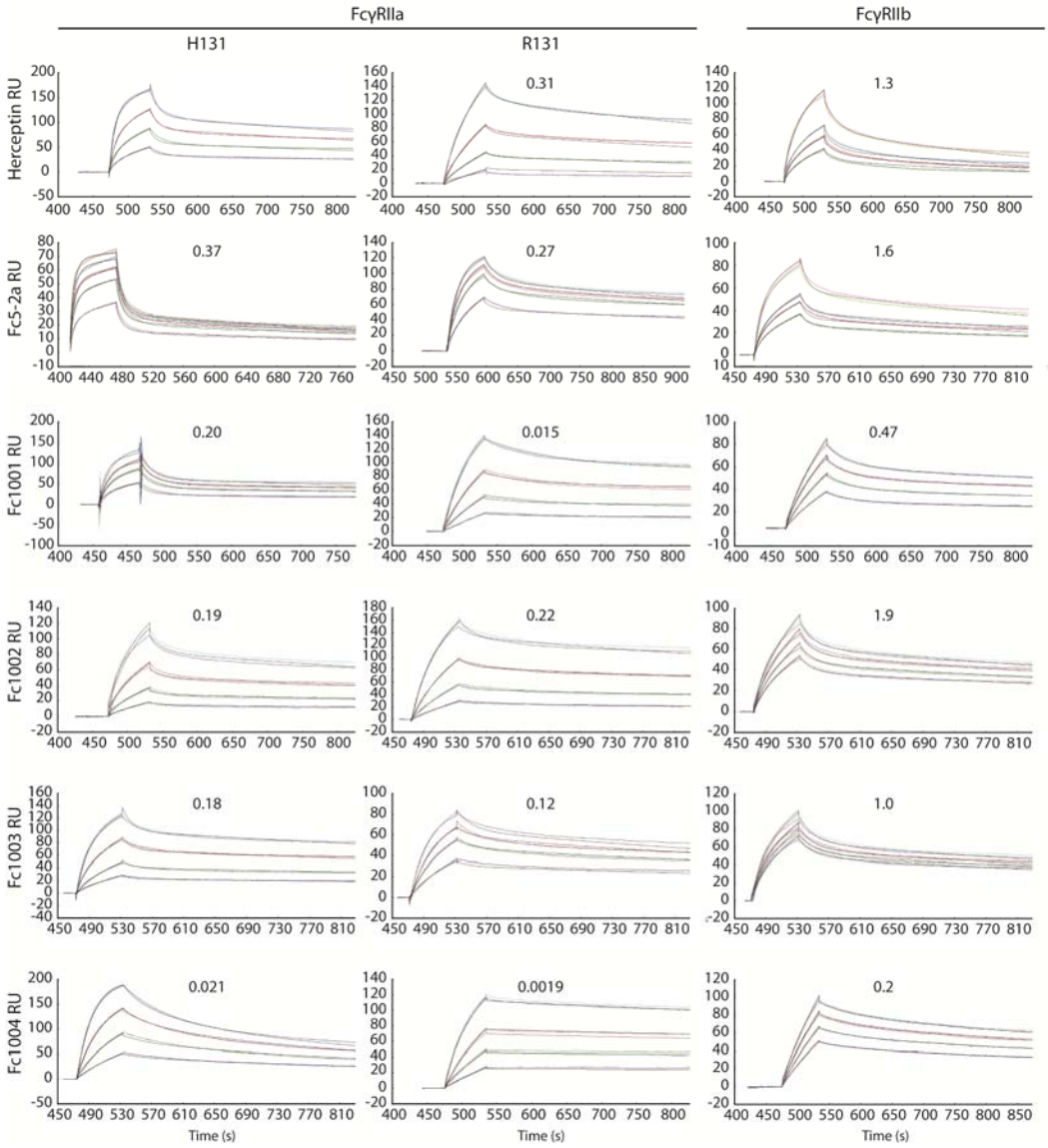

Figure S5. Expression level of Her2 and FcγR on tumor cell lines and macrophages for ADCP assay. (*A*) Her2 expression level on tumor cell lines used for ADCP was confirmed by labeling with 10 µg/ml Herceptin or IgG1 pooled from human serum followed by fluorescent donkey anti-human IgG (H+L) FITC Fab at a 1:50 dilution. Bars are labeled with the immunohistochemical staining category assigned to each tumor cell line (*17*) (*B*) FcγR counts on macrophages were determined using a fluorescent Quantum Simply Cellular bead assay. Macrophages were labeled with 20 µg/ml anti-FcγRI-FITC, 10 µg/ml anti-FcγRIIa-FITC, 1 µg/ml 2B6-N297D-FITC and 20 µg/ml anti-FcγRIII-FITC. (C) Schematic diagram showing the experimental workflow of the ADCP analysis.

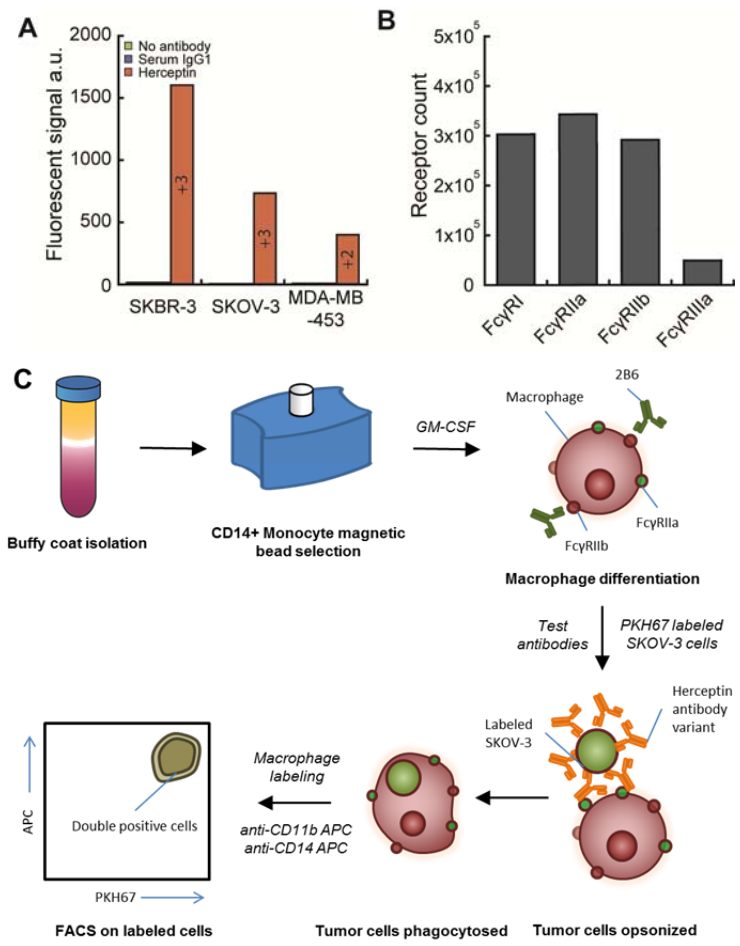

Figure S6. ADCP analysis for ovarian cancer cells expressing medium HER2 density (SKOV-3) and low HER2 density (MDA-MB-453). Tumor cells were labeled with PKH67 membrane dye, opsonized with 0.5 µg/ml antibody and mixed with macrophages at a 1:5 ratio for MDA-MB-453 and 1:10 for SKOV-3 tumor cells. Macrophages were labeled with 10 µg/ml anti-CD11b-APC and 10 µg/ml anti-CD14-APC before FACS interrogation. (*A* - *F*) FACS dot plots for SKOV-3 with No Ab (*A*), AglycoT-N297D (*B*), Herceptin (*C*), GlycoT-G236A (*D*), AglycoT-Fc1001 (*E*), and AglycoT-Fc1004 (*F*). Blue population = macrophages, Red population = SKOV-3 cells, green = double positive phagocytosed SKOV-3 cells. (*G* - *L*) FACS dot plots for MDA-MB-453 with No Ab (*G*), AglycoT-N297D (*H*), Herceptin (*I*), GlycoT-G236A (*J*), AglycoT-Fc1001 (*K*), and AglycoT-Fc1004 (*L*). Blue population = macrophages, Red population = MDA-MB-453 cells, green = double positive phagocytosed MDA-MB-453 cells.

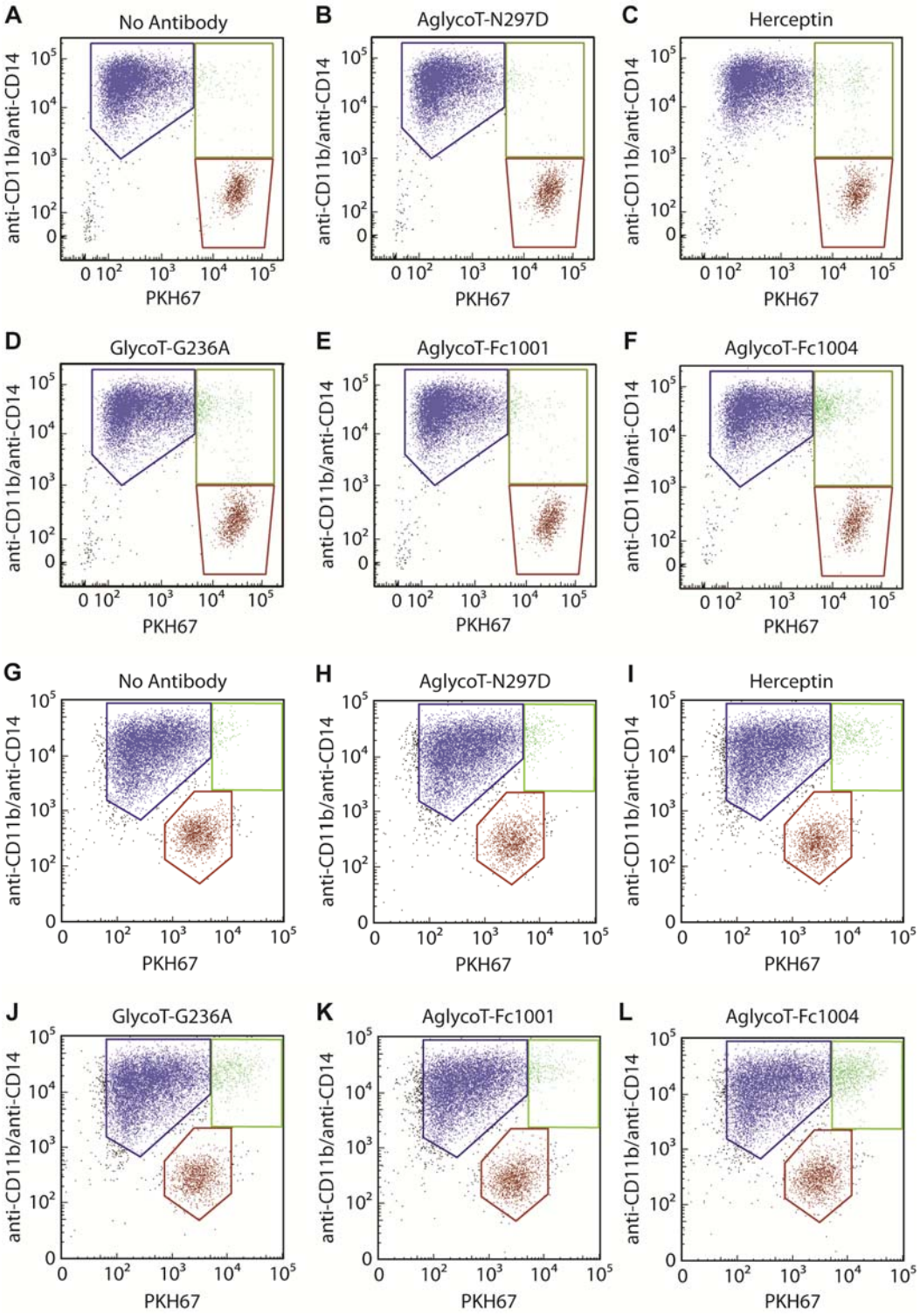
A
No Antibody
B
AglycoT-N297D
C
Herceptin
D
GlycoT-G236A
E
AglycoT-Fc1001
F
AglycoT-Fc1004
G
No Antibody
H
AglycoT-N297D
I
Herceptin
J
GlycoT-G236A
K
AglycoT-Fc1001
L
AglycoT-Fc1004
anti-CD11b/anti-CD14
PKH67

Figure S7. The model returns similar predictions for receptor signaling potency independent of experimental data used for parameterization. (*A* and *B*) ADCP data for Herceptin and AglycoT-Fc1004 were used to obtain intrinsic signaling potency values in the model, which was then used to predict phagocytic response of AglycoT-Fc1001 with both SKOV-3 cells (*A*) and MDA-MB-453 cells (*B*). Blue bars represent experimental values and green bars represent model predictions. (*C* and *D*) ADCP data for AglycoT-Fc1001 and AglycoT-Fc1004 were used to obtain intrinsic signaling potency values in the model, which was then used to predict phagocytic potency of AglycoT-Fc1001 with both SKOV-3 cells (*C*) and MDA-MB-453 cells (*D*). Blue bars represent experimental values and orange bars represent model predictions. (*E*) Predicted phagocytic responses of other Fc variants. Based on $K_{D\_IIa\text{-}H131}$, $K_{D\_IIa\text{-}R131}$, and K_{D_IIb} values from SPR analysis (Table S3), phagocytic response was predicted by the mathematical model for both SKOV-3 cells (dark red bar) and MDA-MB-453 cells (light red bar). Intrinsic signaling potencies for FcγRIIa-H131, FcγRIIa-R131 and FcγRIIb were the same as in Fig. 4 (2.8, 0.4, and -1 respectively).

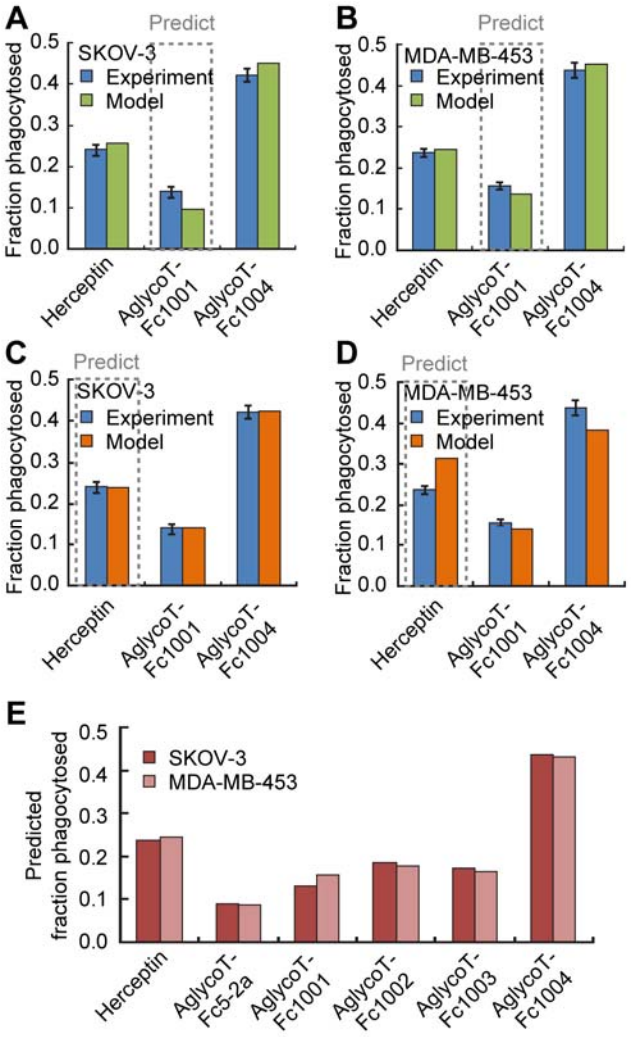
A
Predict
SKOV-3
Experiment
Model
Fraction phagocytosed
0.5
0.4
0.3
0.2
0.1
0.0
Herceptin
AglycoT-Fc1001
AglycoT-Fc1004
B
Predict
MDA-MB-453
Experiment
Model
Fraction phagocytosed
Herceptin
AglycoT-Fc1001
AglycoT-Fc1004
C
Predict
SKOV-3
Experiment
Model
Fraction phagocytosed
Herceptin
AglycoT-Fc1001
AglycoT-Fc1004
D
Predict
MDA-MB-453
Experiment
Model
Fraction phagocytosed
Herceptin
AglycoT-Fc1001
AglycoT-Fc1004
E
SKOV-3
MDA-MB-453
Predicted fraction phagocytosed
0.5
0.4
0.3
0.2
0.1
0.0
Herceptin
AglycoT-Fc5-2a
AglycoT-Fc1001
AglycoT-Fc1002
AglycoT-Fc1003
AglycoT-Fc1004